vol. MTT-23, pp. 828–831, Oct. 1975.
[17] W. K. Gwarek, "Nonlinear analysis of microwave mixers," M.S. thesis, MIT, Cambridge, Sept. 1974.
[18] S. O. Rice, "Mathematical analysis of random noise," *Bell Syst. Tech. J.*, vol. 23, no. 3, pp. 282–332, July 1944.
[19] V. R. Bennet, *Electrical Noise*. New York: McGraw-Hill, 1960.
[20] D. R. Decker and S. Weinreb, private communication.
[21] S. M. Sze, *Physics of Semiconductor Devices*. New York: Wiley, 1969 (see p. 90 *et seq.*).
[22] W. Baechtold, "Noise behavior of GaAs field-effect transistors with short gates," *IEEE Trans. Electron Devices*, vol. ED-19, pp. 674–680, 1972.
[23] D. N. Held, "Analysis of room temperature millimeter-wave mixers using GaAs Schottky barrier diodes," Sc.D. dissertation, Department of Electrical Engineering, Columbia University, New York, 1976.
[24] J. A. Calviello, J. L. Wallace, and P. R. Bie, "High performance GaAs quasi-planar varactors for millimeter waves," *IEEE Trans. Electron Devices*, vol. ED-21, pp. 624–630, Oct. 1974.

Conversion Loss and Noise of Microwave and Millimeter-Wave Mixers: Part 2—Experiment

DANIEL N. HELD, MEMBER, IEEE, AND ANTHONY R. KERR, ASSOCIATE MEMBER, IEEE

Abstract—**The theory of noise and conversion loss in millimeter-wave mixers, developed in a companion paper, is applied to an 80–120-GHz mixer. Good agreement is obtained between theoretical and experimental results, and the source of the recently reported "anomalous noise" is explained. Experimental methods are described for measuring the embedding impedance and diode equivalent circuit, needed for the computer analysis.**

I. Introduction

In Part 1 of this paper [1] the theory of microwave and millimeter-wave mixers was presented in a form suitable for analysis by digital computer. The present paper gives the results of such an analysis, comparing computed and measured conversion loss, noise, and output impedance for an 80–120-GHz mixer under various operating conditions.

The significance of this work in relation to earlier work is discussed in the introduction to Part 1, the salient points being that this method of analysis gives unprecedented agreement between theory and experiment and that the "anomalous noise" [2] reported in millimeter-wave mixers is entirely accounted for.

The analysis requires a knowledge of the embedding impedance seen by the diode at a finite number of frequencies, and of the equivalent circuit of the diode, including noise sources. Experimental methods for determining these input quantities are described in Sections II and III. The mixer analysis is described in Section IV and typical sets of theoretical and measured results are shown to be in good agreement. Section V discusses the sources of mixer noise and loss, and small-signal power flow in the mixer.

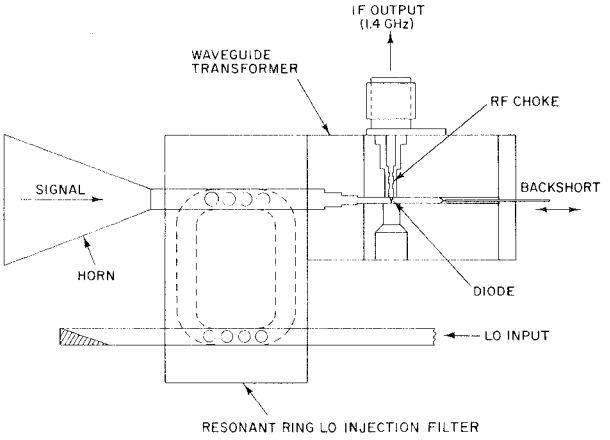

Fig. 1. Cross-section of the 80–120-GHz mixer used in this work.

The mixer used for these experiments is the room-temperature 80–120-GHz mixer described in [3] and is shown here in Fig. 1. It uses a 2.5-μm-diameter GaAs Schottky diode in a quarter-height waveguide mount. The diode was made by Professor R. J. Mattauch at the University of Virginia.

Manuscript received February 18, 1977; revised May 12, 1977.

D. N. Held was with the Department of Electrical Engineering, Columbia University, New York, NY 10027. He is now with the Jet Propulsion Laboratory, California Institute of Technology, Pasadena, CA 91103.

A. R. Kerr is with the NASA Institute for Space Studies, Goddard Space Flight Center, New York, NY 10025.

0018-9480/78/0200-0055$00.75

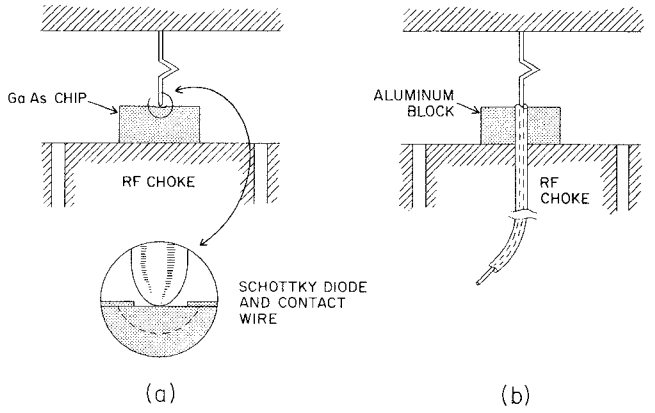

Fig. 2. Technique for measuring the embedding impedance seen by the diode. The diode in the real mixer (a) is replaced in the scale model (b) by the end of a small coaxial cable through which the embedding impedance can be measured directly.

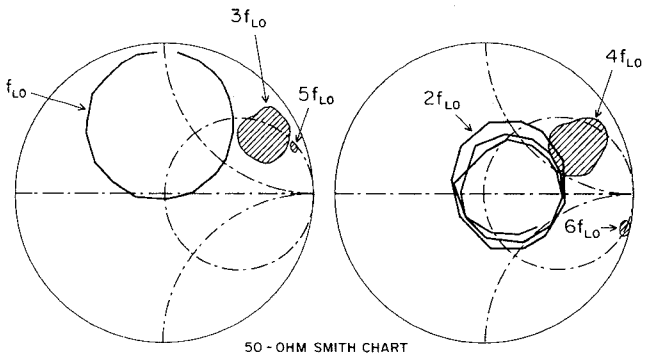

Fig. 3. The embedding impedance at harmonics of the LO frequency, for $f_{LO} = 87$ GHz. The impedances are shown as functions of backshort position.

II. The Diode Embedding Impedance

Eisenhart and Kahn [4], [5] have described a technique whereby it is possible to measure the embedding impedance seen by a waveguide-mounted diode. The diode is removed from its mount and replaced by a small coaxial cable, so the impedance seen by the end of the cable is essentially equal to the embedding impedance normally seen by the diode. The other end of the cable is connected to a slotted line or network analyzer which measures this impedance. Except for some small corrections due to differences in geometry in the region immediately surrounding the diode, the technique directly provides the desired embedding impedance. In order to make this technique practical for millimeter-wave mixer mounts, it is necessary to perform the measurements on a large-scale model of the mixer.

For the 80–120-GHz mixer used as an example in this paper, a 65 × scale model was constructed, including the stepped waveguide transformer, diode mount, RF choke, and backshort, shown in Fig. 1. The input waveguide was terminated in a matched multimode waveguide load, and the GaAs diode chip was modeled by an aluminum block as shown in Fig. 2. Using a Hewlett-Packard 8410A network analyzer it was then possible to measure the embedding impedance up to the sixth harmonic of the local oscillator. Because of the geometrical differences between the diode and the coaxial measuring probe, the measured embedding impedance had to be corrected for fringing effects. Equivalent circuits for the region close to the diode in the actual mixer and in the diode-less model are derived in [6], where it is shown that the correction to the measured embedding impedance is equivalent to adding a 0.63 fF (0.00063 pF) capacitor in shunt with the measured impedance (cf. the zero-bias diode capacitance $\mathscr{C}_{j0} \simeq 7.0$ fF).

Typical embedding impedances measured at the scale-model equivalent of 87 GHz are illustrated in Fig. 3. The experimental results illustrated in this figure are presented as a function of the mixer backshort position, since in subsequent sections of this paper mixer performance will be evaluated as a function of backshort position. It is clear from Fig. 3 that the embedding impedances at the harmonics of the local oscillator cannot be considered as open-circuits, short-circuits, or even simple reactive terminations, as has sometimes been assumed in the literature. In particular, the embedding impedance at the second harmonic has a substantial and widely varying real part.

III. The Diode Equivalent Circuit

In Section V of Part 1 the characteristics of very small Schottky diodes were discussed. It was pointed out that the RF skin effect could contribute substantially to the series resistance, while nonuniform epilayer doping and fringing effects at the periphery of the depletion layer might cause the capacitance-law exponent γ to be voltage-dependent. It was further pointed out that scattering, observed in Schottky diodes at high-current levels, would effect mixer noise, and that thermal time constants must be taken into account when measuring the series resistance of a diode.

The equivalent circuit of a Schottky barrier diode, including noise sources, is shown in Fig. 4. In the following paragraphs procedures are described for determining the element values of this equivalent circuit, which are appropriate at millimeter wavelengths.

A. Junction Capacitance

The capacitance of the junction as a function of voltage is given by [7]

$$\mathscr{C}_j(v_j) = \frac{dQ}{dv_j} = \mathscr{C}_{j0}\left(1 - \frac{v_j}{\phi}\right)^{-\gamma(v_j)} \tag{1}$$

where $\mathscr{C}_{j0}$ is the zero-voltage capacitance, ϕ is the barrier potential, and $\gamma(v_j)$ is related to the geometry of the junction and the semiconductor doping profile. If the junction can be considered planar, with negligible fringing effects, and if the epilayer doping is uniform, then $\gamma = 0.5$. However, when the diameter of the diode is not large compared with the thickness of the depletion layer, fringing effects at the edges of the diode may be significant, and will be most pronounced under reverse bias when the depletion layer is widest.

The junction capacitance can be measured at 1 MHz

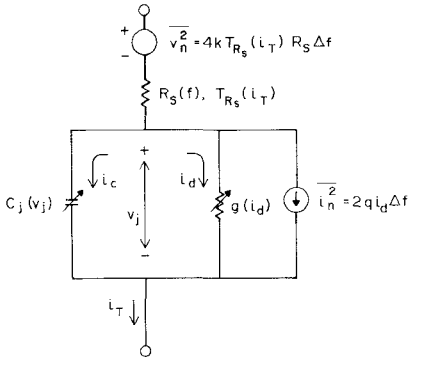

TYPICAL VALUES FOR
2.5μ Ga As DIODES

i_O	8.3×10^{-17}A
η	1.05
C_{jO}	7×10^{-15} F
ϕ	0.95 V
$R_{S\,DC}$	9.4Ω
$R_{S_{1\text{-}15GHz}}$	12–16Ω
$\gamma(V_j)$	0.3 → 0.5
$T_{R_S}(i_T)$	>298°K

Fig. 4. The equivalent circuit of a Schottky diode, including frequency dependent series resistance and current dependent resistor noise temperature.

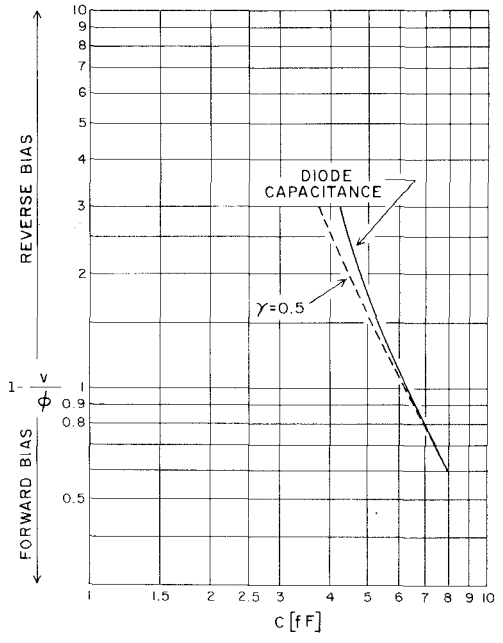

Fig. 5. Experimental $\mathscr{C}_j$ versus $(1 - v_j/\phi)$ for a typical 2.5-μm diode, illustrating the voltage dependence of γ.

using a capacitance bridge[1] [6], [8]. By plotting log $\mathscr{C}_j$ versus log $(1 - v_j/\phi)$, a line whose slope is equal to $-\gamma$ is obtained. Experimental results indicate that the value of γ for some diodes exhibits a pronounced voltage dependence, a typical result being shown in Fig. 5.

The question arises as to whether the capacitance measured at 1 MHz is meaningful at 100 GHz and above. There is, however, no evidence to suggest any frequency

[1] A Boonton model 75D was used for this work.

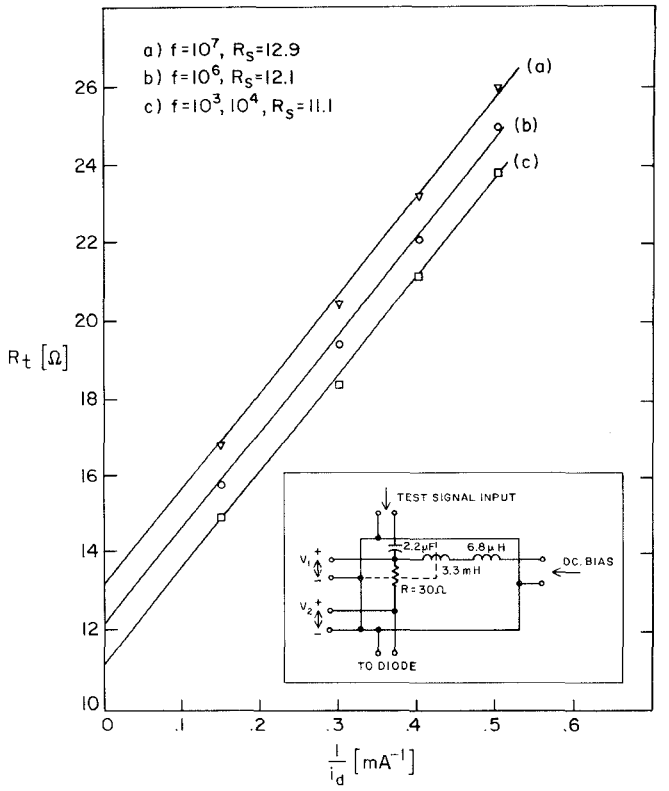

Fig. 6. Measured incremental resistance of a 2.5-μm gallium arsenide diode as a function of reciprocal dc bias current, showing apparent frequency dependence of the series resistance (the y-axis intercept). This is due to heating effects. Inset: Circuit of device for measuring the incremental resistance R_t at frequencies up to 10 MHz.

dependence of the junction capacitance over this range of frequencies. There have been some papers [10]–[12] dealing with the effect of deep-level donors on frequency dependence of the transition capacitance of p-n junctions. However, the effect is only significant when the number of deep traps is comparable to the number of donors, which should not be the case for the heavily doped diodes under study. A second factor which can cause a frequency dependence of the junction capacitance is the scattering limited velocity of the electrons in the semiconductor. This limits the rate at which the depletion layer can be depleted or refilled, and is expected to have negligible effects below ~ 100 GHz [13].

B. The Barrier Resistance and the Series Resistance

It has been shown by Weinreb and Decker [14] that the conventional method of determining the series resistance R_s from the dc log I–V curve contains an inherent error due to heating at the junction. To determine the true value of R_s measurements must be performed at frequencies greater than the reciprocal of the shortest thermal time constant of the diode and its mount. Measurements of these thermal time constants [14] indicate that errors should be negligible above ~ 20 MHz.

A simple circuit, shown in Fig. 6, enables the incremental resistance R_t of a forward-biased diode to be measured in the frequency range 1 kHz–10 MHz. Measurements on a 2.5 μm GaAs diode indicate that the resistance starts to increase above ~30 kHz and levels off at ~10 MHz. These

results are shown in Fig. 6 where R_t is plotted as a function of reciprocal bias current for several different frequencies; the value of R_s at each frequency is given by the y-axis intercept. It is seen that the resistance increases by ~ 2–$3\ \Omega$ between 10 kHz and 10 MHz. Further confirmation of these measurements comes from Weinreb and Decker [14] who measured the thermal time constants of the diode chip and mounting structure and found them to be approximately 1 μs and 50 ms, respectively.

Another important phenomenon effecting the diode's series resistance is the RF skin effect. This effect occurs predominantly in the degenerately doped substrate of the diode chip and in the contacting whisker. The skin resistance has been calculated by several investigators [15], [16], [6] and for a 2.5-μm diode is generally conceded to add about 2–3 Ω to the series resistance at 100 GHz. Direct measurement of the series resistance of a waveguide-mounted diode was performed using a new technique described in [6]. Values obtained for the series resistance at 115 GHz were typically 2 Ω larger than the low frequency values[2] as expected.

The results of these measurements of the series resistance are summarized in Table I. It is clear that the series resistance at millimeter wavelengths may be as much as twice the value obtained by the conventional dc method.

TABLE I
SERIES RESISTANCE VALUES

R_s measured at DC (including thermal effects)	6.8±0.1 ohm
R_s measured at 10 MHz	9.4±0.2 ohm
Thermal time-constant error	-2.6±0.3 ohm
True low frequency R_s (measured at 10 MHz)	9.4±0.2 ohm
Calculated skin-effect at 115 GHz	2.5±0.5 ohm
Predicted value of R_s at 115 GHz	11.9±0.7 ohm
Measured value of R_s at 115 GHz	11.2±2.0 ohm

C. Noise Temperature of the Series Resistance

It is well known that at electric field strengths in the vicinity of 3×10^3 V/cm^3, bulk GaAs displays a nonlinear I–V characteristic which is due primarily to central valley and intervalley phonon scattering.[3] It will be shown in Section IV that under normal mixer operating conditions the instantaneous value of the current through the series resistance of a diode can reach levels ~ 10 mA. For the diodes used in this work it can be shown that the peak value of the electric field in the undepleted epitaxial material may then be as large as 1.9×10^3 V/cm.[4] Although this value is comfortably below the critical field required for the onset of the Gunn effect at low frequencies, the field strength is sufficient to increase substantially the effective temperature of the electron gas in the GaAs and hence the noise temperature of the series resistance.

The noise temperature of the series resistance, measured at a frequency of 1.4 GHz on a dc biased diode, is shown in Fig. 7 as a function of the dc current. The noise temperature of the series resistance was derived by measuring the diode output temperature and correcting for the effect of the shot noise produced in the junction [6], [17]. Also shown in Fig. 7 are results reported by Baechtold [18] who measured the noise temperature of a bulk sample of GaAs. It is clear, then, that at high currents excess noise is generated in GaAs mixer

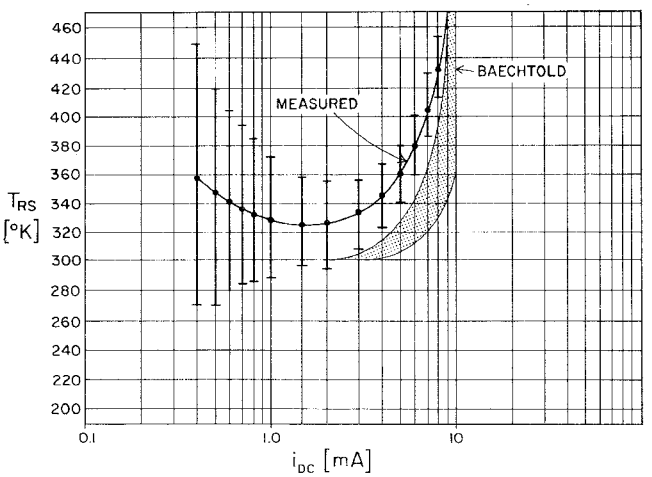

Fig. 7. Noise temperature of the series resistance at 1.4 GHz as a function of dc current. Also shown are Baechtold's results for an epilayer doping between 2 and 3×10^{17} cm^{-3} (shaded region).

diodes due to scattering phenomena. Although the scattering noise has been measured at 1.4 GHz, the results should be valid in the millimeter-wave region since the effective intervalley scattering time constant in GaAs is on the order of 2×10^{-12} s [19]–[21], and the central valley scattering time constant is assumed to be short compared with the dielectric relaxation time of the epitaxial layer which is $\sim 10^{-14}$ s [22], indicating a spectral density which is essentially uniform up to approximately 80 GHz, decreasing at higher frequencies.

When the diode is operating as a mixer the noise temperature of the series resistance will be a function of time, and the down-converted components of this noise will be partially correlated [1]. For a room-temperature mixer this correlation is expected to have a small effect, and it will be assumed here that scattering noise can be approximated by an increased average noise temperature of the series resistance,[5] an assumption supported by the good agreement obtained between theory and experiment in Section

[2] Low-frequency values corrected for thermal time-constant effects.

[3] The critical field for highly doped GaAs is approximately 5×10^3 V/cm [9], [18].

[4] This figure is based on the assumption of uniform current flow through a 2.5-μm diameter diode, with a resistivity of 0.096 Ω-cm in the epilayer, corresponding to an impurity concentration of 2.5×10^{17}/cm^3.

[5] The average noise temperature is derived by integrating the measured noise temperature (Fig. 7) at the total diode current, i_T (Fig. 8), over the LO cycle. Typical average noise temperatures are approximately 60 K–100 K above ambient at room temperature.

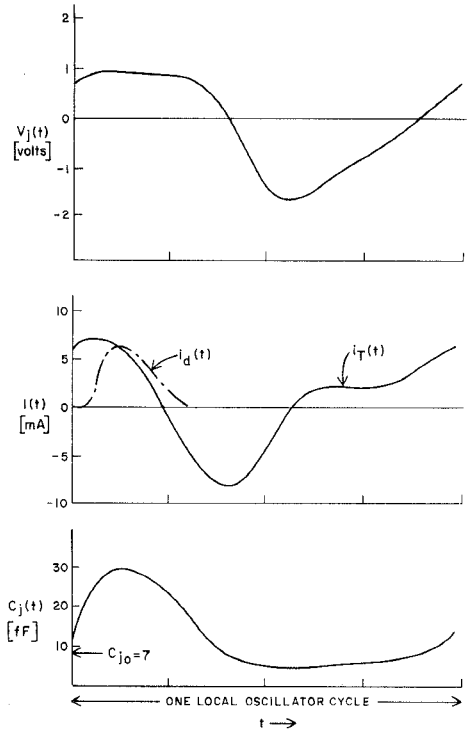

Fig. 8. Typical diode waveforms at 87 GHz. The junction voltage $v_j(t)$, total current in R_s, $i_T(t)$, current in the diode conductance, $i_d(t)$, and junction capacitance $\mathscr{C}_j(t)$ are illustrated for a single local oscillator cycle. The dc bias conditions are: $I_{dc} = 2.0$ mA, $V_{dc} = 0.5$ V.

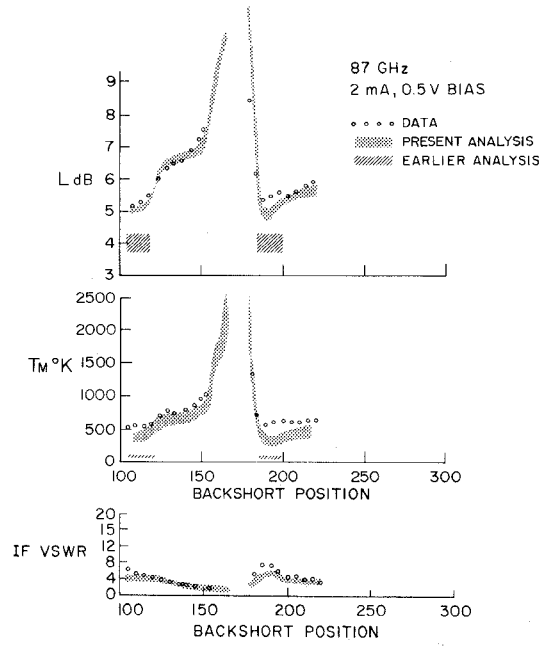

Fig. 9. Comparison of theoretical and experimental results at 87 GHz. The SSB conversion loss L, equivalent SSB input noise temperature T_M of the mixer (excluding IF amplifier noise), and IF VSWR with respect to 50 Ω, are shown as functions of backshort position. The theoretical results are computed for a broadband mixer (equal signal and image response) with the capacitance exponent $\gamma = 0.3$–0.5 and the series resistance $R_S(100\text{ GHz}) = 12$–16 Ω. Also shown are the results of an earlier analysis [2], [3] which led to the observation of anomalous mixer noise. T_M is related to the noise temperature ratio t of a broad-band mixer by $T_M = T_a(Lt - 2)$, where T_a is the ambient temperature of the mixer and its input termination.

IV. In cryogenic mixers however, scattering noise and its partially correlated down-converted components are expected to be very significant and this simplifying assumption may be quite invalid.

IV. Mixer Performance Analysis

It was shown in Part 1 [1] that if the embedding impedance and the equivalent circuit of the diode are known, it is possible to solve the large-signal nonlinear problem to determine the LO waveforms at the diode, and then to determine the small-signal conversion loss and noise figure of the mixer. In this section the results of such an analysis are given for the 80–120 GHz mixer shown in Fig. 1 [3]. The embedding impedance was measured on a model, as described in Section II of the present paper, and the large-signal LO waveforms were computed as described in Section II of Part 1. Typical waveforms are shown in Fig. 8.

Knowing the LO waveforms, the conversion loss and noise temperature of the mixer can be determined as described in Sections II and III of Part 1. Since the mixer backshort setting has the strongest effect of all the external variables on mixer performance (other variables are dc bias and LO power), the measured and computed results given here are plotted as functions of backshort position. This serves not only to verify the accuracy of the computed solution for a wide variety of embedding impedances, but also provides useful insight into the behavior of the mixer. Typical sets of results are shown in Figs. 9 and 10 for 87 and 115 GHz. Computed results are shown for $\gamma = 0.3$–0.5 and $R_s(100\text{ GHz}) = 12$–$16\ \Omega$; these correspond to the likely range of values of these quantities allowing for skin effect and fringing effects as discussed in Section III. It has been assumed in this work that $\gamma(v_j)$ can be approximated by a voltage-independent mean value and that R_s exhibits the normal skin-effect type of frequency dependence. Also shown in Fig. 9 are the results of an earlier analysis [2], [3] which led to the observation of an anomalous component of mixer noise, thereby stimulating the present work.

The main sources of error in the computed results are expected to be due to high-Q effects and to loss in the backshort. It was assumed for simplicity that the embedding impedance at a LO harmonic was equal to the impedance at the adjacent sideband frequencies, i.e., $Z_e(n\omega_p \pm \omega_{if}) = Z_e(n\omega_p)$. Clearly this assumption will lead to errors if there are any sharp features on the loss or noise-temperature curves of Figs. 9 and 10. The conversion-loss minimum in Fig. 10 is an example of this and it can be seen that the measured and computed results differ most in this region. The backshort used in the experimental mixer was of the contacting spring-finger type, generally assumed to have low loss. Measurement of the loss of this particular backshort revealed a surprisingly large loss, equivalent to a resistance of $\sim 8\ \Omega$ at the plane of the short-circuit. At certain backshort positions this can contribute substantially to the measured conversion loss. Experimental repeatability was somewhat degraded by this backshort, presumably due to poor electrical contact with the waveguide. Experience during these measurements suggests experimental uncer-

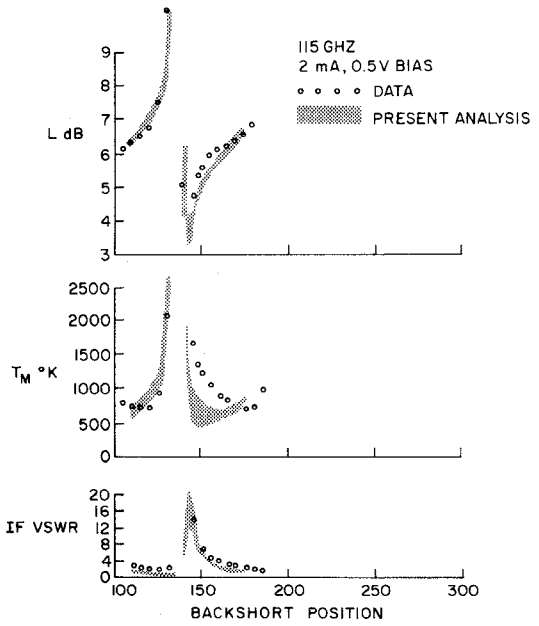

Fig. 10. Comparison of theoretical and experimental mixer performance at 115 GHz. See Fig. 9 caption for details.

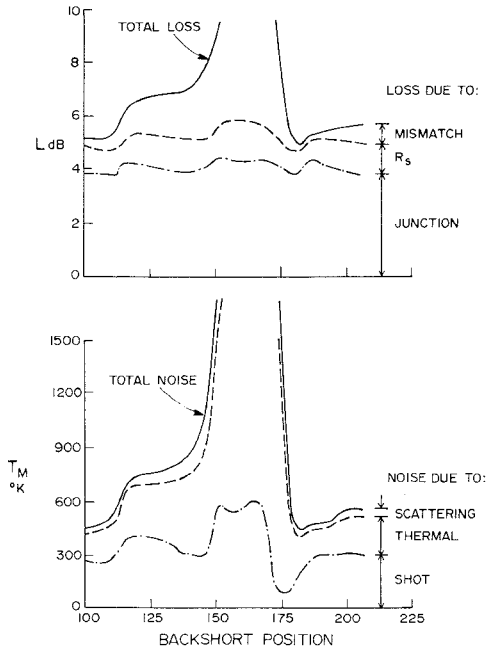

Fig. 11. Breakdown of mixer loss and noise at 87 GHz.

tainties of ± 0.3 dB in L and $\pm 130°$ in T_M for most backshort settings, doubling in the vicinity of the sharp conversion-loss minimum. All measurements were performed using the 1.4-GHz IF radiometer/reflectometer apparatus described by Wienreb and Kerr [23].

V. Discussion

Having established that the performance of a mixer can be accurately predicted by the theory given in the companion paper [1], it is useful to evaluate the various contributions to the conversion loss and the mixer noise.

A. Sources of Mixer Loss and Noise

In Fig. 11 T_M and L are shown broken down into their constituant parts. The three major components of the conversion loss are 1) RF input mismatch loss, 2) dissipation in the series resistance at the signal and intermediate frequencies, and 3) loss in the junction, which includes power dissipated in the junction resistance at the signal and intermediate frequencies and also power lost by conversion to other frequencies. It should be noted that the mismatch loss can not necessarily be eliminated by RF tuning, since for broadband mixers the minimum overall conversion loss usually occurs for a mismatched input [24].

Noise in this room-temperature mixer is composed almost entirely of shot and thermal noise; the effect of the scattering mechanisms is fairly small. In the vicinity of the minimum of T_M the contributions from the shot and thermal sources are comparable.

B. Power Flow in the Mixer

From the conversion loss analysis given in Part 1 it is possible to calculate the conversion loss between any two frequencies and to analyze the power flow in the mixer. A typical result is shown in Fig. 12 for two backshort positions at 115 GHz. It is interesting to observe from Fig. 12(a)

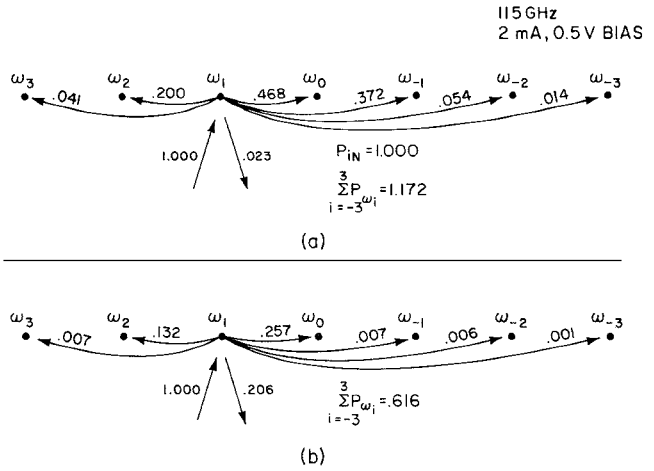

Fig. 12. Power flow at 115 GHz for two backshort positions. (a) Backshort position corresponding to minimum conversion loss. (b) Backshort position corresponding to minimum T_M.

that the mixer can behave as an active device, more small signal power being generated at the sideband frequencies than is incident at the signal frequency. This is a consequence of the time variation of the junction capacitance which produces "parametric" effects. It is also interesting to note that a substantial amount of power is dissipated at the sum frequency $\omega_2 = 2\omega_p + \omega_0$. Thus the embedding impedance at that frequency may be as important in mixer design as is the termination of the image frequency.

VI. Conclusion and Summary

The theory given in Part 1 has been used to predict the conversion loss and noise of an 80–120-GHz mixer. Close agreement was obtained between measured and computed results for a variety of operating conditions. The analysis has demonstrated the following.

1) For a room temperature mixer the "anomalous" noise can be explained almost entirely by shot and thermal noise. The contribution due to scattering is typically only 10 percent.

2) The shot noise has components which, when down converted via the action of the mixer, are correlated.

3) The assumptions that the series resistance is time invariant and that scattering noise can be approximated by an increase in the noise temperature of the series resistance, are reasonable for this room-temperature mixer. This is not expected to be the case for cryogenic mixers, however, as scattering noise may be a substantial part of the overall noise.

4) The value of the series resistance in the vicinity of 100 GHz may be as much as twice its apparent dc value. This is due to the RF skin effect, and to an error, caused by thermal effects, inherent in the conventional method of determining the low-frequency series resistance from the dc log I–V characteristic of the diode. The difference between the apparent dc series resistance and the actual RF value accounts for approximately 1 dB of passive loss in the mixer used in this work.

Acknowledgment

The authors wish to thank the following for their substantial contributions to the work reported here: R. J. Mattauch and G. Green of the University of Virginia; S. Weinreb and D. R. Decker of the National Radio Astronomy Observatory; S. P. Schlessinger and E. Yang of Columbia University; and P. Thaddeus, J. Grange, I. Silverberg, and H. Miller of the Goddard Institute for Space Studies.

References

[1] D. N. Held and A. R. Kerr, "Conversion loss and noise of microwave and millimeter-wave mixers: Part 1—Theory," *IEEE Trans. Microwave Theory Tech.*, vol. MTT-26, Feb. 1978.

[2] A. R. Kerr, "Anomalous noise in Schottky diode mixers at millimeter wavelengths, *IEEE MTT-S Int. Microwave Symp., Digest of Technical Papers*, 1975.

[3] ——, "Low-noise room-temperature and cryogenic mixers for 80–120 GHz," *IEEE Trans. Microwave Theory Tech.*, vol. MTT-23, pp. 781–787, 1975.

[4] R. L. Eisenhart, "Impedance characterization of a waveguide microwave circuit," U.S. Army Electronics Command, Fort Monmouth, NJ, Technical Report 208, 1971.

[5] R. L. Eisenhart and P. J. Kahn, "Theoretical and experimental analysis of a waveguide mounting structure," *IEEE Trans. Microwave Theory Tech.*, vol. MTT-19, pp. 706–719, 1971.

[6] D. N. Held, "Analysis of room temperature millimeter-wave mixers using GaAs Schottky barrier diodes," Sc.D. dissertation, Columbia University, 1976.

[7] S. M. Sze, *Physics of Semiconductor Devices*. New York: Wiley, 1969.

[8] A. R. Kerr, R. J. Mattauch, and J. Grange, "A new mixer design for 140–220 GHz," *IEEE Trans. Microwave Theory Tech.*, vol. MTT-25, pp. 399–401, May 1977.

[9] R. J. Mattauch, Private communication.

[10] E. Schibli and A. G. Milnes, "Effects on deep impurities on n + p junction reverse-biased small-signal capacitance," *Solid State Electron.*, vol. 11, pp. 323–334, 1968.

[11] W. Schultz, "A theoretical expression for the impedance of reverse-biased P-N junctions with deep traps," *Solid State Electron.*, vol. 14, pp. 227–231, 1971.

[12] K. Hesse and H. Strack, "On the frequency dependence of GaAs Schottky barrier capacitances," *Solid State Electron.*, vol. 15, pp. 767–774, 1972.

[13] J. C. Irvin, T. P. Lee, and D. R. Decker, "Varactor diodes," ch. in *Microwave Semiconductor Devices and their Circuit Application*, H. A. Watson, ed. New York: McGraw-Hill, 1969.

[14] S. Weinreb and D. R. Decker, Private communication.

[15] J. A. Calviello, J. L. Wallace, and P. R. Bie, "High performance GaAs quasi-planar varactors for millimeter waves," *IEEE Trans. Electron Devices*, vol. ED-21, pp. 624–630, Oct. 1974.

[16] M. Schneider, Private communication.

[17] R. J. Mattauch and T. J. Viola, "High frequency noise in Schottky barrier diodes," *Research Laboratories for the Engineering Sciences*, Univ. of Virginia, Report No. EE-4734-101-73U, 1973.

[18] W. Baechtold, "Noise behavior of GaAs field-effect transistors with short gates," *IEEE Trans. Electron Devices*, vol. ED-19, pp. 674–680, 1972.

[19] B. Culshaw and P. A. Blakey, "Intervalley scattering in gallium arsenide avalanche diodes," *Proc. IEEE (Lett.)*, vol. 64, pp 569–571, 1976.

[20] T Ohmi, "A limitation on the frequency of Gunn effect due to the intervalley scattering time," *Proc. IEEE (Lett.)*, vol. 55, pp. 1739–1740, 1967.

[21] V. Szekely and K. Tarnay, "Intervalley scattering model of the Gunn domain," *Electronics Letters*, vol. 4, pp. 592–594, 1968.

[22] D. E. McCumber and A. G. Chynoweth, "Theory of negative conductance amplification and of Gunn instabilities in 'two-valley' semiconductors," *IEEE Trans. Electron Devices*, vol. ED-13, pp. 4–21, 1966.

[23] S. Weinreb and A. R. Kerr, "Cryogenic cooling of mixers for millimeter and centimeter wavelengths," *IEEE Journal Solid State Circuits*, vol. SC-8, pp. 58–63, 1973.

[24] A. A. M. Saleh, *Theory of Resistive Mixers*. Res. Monograph 64. Cambridge, MA: MIT Press, 1971.